



RESEARCH LETTER

10.1029/2023GL107549

Unveiling the Hidden Threat: Drought-Induced Inelastic Subsidence in Expansive Soils

Jennifer Welch¹, Guoquan Wang¹ , Yan Bao², Shuangcheng Zhang³ , Guanwen Huang³, and Xie Hu⁴ 

¹Department of Earth and Atmospheric Sciences, University of Houston, Houston, TX, USA, ²Key Laboratory of Urban Security and Disaster Engineering of Ministry of Education, Beijing University of Technology, Beijing, China, ³School of Geology Engineering and Geomatics, Chang'an University, Xian, China, ⁴College of Urban and Environmental Sciences, Peking University, Beijing, China

Key Points:

- Prolonged droughts cause up to 2 dm of subsidence in shallow expansive soils (<4 m deep) in Galveston, TX, 10% of which is inelastic
- Prolonged droughts lead to notable subsidence in open fields with expansive soils, but less in built-up areas or non-expansive soil areas
- Recurring droughts lead to permanent land elevation losses in open-field coast, possibly skewing sea-level rise and flood risk projections

Correspondence to:

G. Wang,
gwang@uh.edu

Citation:

Welch, J., Wang, G., Bao, Y., Zhang, S., Huang, G., & Hu, X. (2024). Unveiling the hidden threat: Drought-induced inelastic subsidence in expansive soils. *Geophysical Research Letters*, 51, e2023GL107549. <https://doi.org/10.1029/2023GL107549>

Received 30 NOV 2023

Accepted 18 MAR 2024

Author Contributions:

Conceptualization: Guoquan Wang

Formal analysis: Guoquan Wang, Shuangcheng Zhang

Investigation: Jennifer Welch,

Guoquan Wang, Yan Bao,

Guanwen Huang, Xie Hu

Methodology: Jennifer Welch,

Guoquan Wang, Shuangcheng Zhang,

Guanwen Huang, Xie Hu

Project administration: Jennifer Welch,

Guoquan Wang

Writing – original draft: Guoquan Wang,

Xie Hu

Writing – review & editing:

Jennifer Welch, Guoquan Wang, Yan Bao,

Shuangcheng Zhang, Guanwen Huang

Abstract Expansive soils pose a significant challenge in geotechnical engineering, especially in coastal areas. While research has mainly focused on their elastic properties, this study explores the overlooked aspect of inelastic subsidence during prolonged droughts, utilizing decade-long GPS datasets from the University of Houston Coastal Center. Our findings reveal substantial subsidence, approximately one to two dm, during the summer droughts of 2018, 2020, 2022, and 2023, due to compaction within the upper 4 m of expansive soils. Inelastic subsidence constitutes roughly 10% of the total subsidence, resulting in step-like permanent land elevation loss over time. Notably, drought-induced subsidence is prominent in open-field areas with expansive soils but is minor in built-up areas or in non-expansive soil regions. The occurrence of inelastic subsidence challenges traditional assessments of relative sea-level rise and coastal flooding, emphasizing the need to consider it in coastal infrastructure planning for enhanced resilience against climate uncertainties.

Plain Language Summary Expansive soils, often found in coastal regions, are known for causing issues like land shifts and unstable buildings. Our research adds a new dimension: prolonged droughts can lead to significant, irreversible sinking of expansive soils, permanently lowering the elevation of open land areas. Using a decade of GPS data, we found that during droughts, these soils can sink considerably and will not fully recover. Interestingly, in developed regions where pavement covers the soils, thereby minimizing moisture loss, this sinking is observed to be minimal. In the Galveston coastal area, drought-induced sinking can reach one to two dm, with irreversible subsidence making up about 10% of the total subsidence. This becomes a growing concern as droughts become more frequent due to climate change, especially in coastal areas. Additionally, our results suggest that current methods for estimating sea-level rise may be missing a key factor: we have underestimated the speed at which uninhabited coastal lands are sinking because we did not account for this irreversible sinking due to droughts.

1. Introduction

Expansive soils, often dominated by clay minerals, can undergo significant volume changes in response to fluctuations in soil moisture. During periods of high moisture, these soils swell, expanding their volume and exerting significant pressure on surrounding structures. Conversely, in times of prolonged drought, they desiccate, contracting and causing subsidence, which is often regarded as elastic deformation, recoverable after the drought. Inelastic deformation refers to the permanent change in the volume or shape of the soil that does not revert back to its original state, even after the removal of the cause of deformation, such as drought.

Elastic deformation often retains large amplitudes and has immediate impacts on structures and infrastructure. There are significant studies about the elastic deformation of expansive soils under varying moisture conditions in geotechnical engineering, often referred to as seasonal subsidence and heave (e.g., Barthélémy et al., 2023; Charpentier et al., 2022; Kai et al., 2020; Mostafiz et al., 2021; Wang, 2022a). These studies have been pivotal in understanding soil behavior under drought conditions and their corresponding damage to buildings and infrastructures. By analyzing the soil-structure interaction during these seasonal changes, researchers have been able to propose innovative solutions for foundation designs that adapt to the dynamic nature of expansive soils.

In contrast, the inelastic deformation of expansive soils, while less visible and of minor magnitude, has not been widely recognized as an engineering concern due to its minimal impact on buildings, and as a result, it is often

© 2024. The Authors.

This is an open access article under the terms of the [Creative Commons Attribution License](https://creativecommons.org/licenses/by/4.0/), which permits use, distribution and reproduction in any medium, provided the original work is properly cited.

overlooked and has yet to emerge as a recognized area of study. However, it can result in permanent loss of land surface elevation and result in long-term detrimental effects, particularly in coastal areas. Here, permanent land subsidence can exacerbate the vulnerability to sea-level rise and increase the likelihood of flooding, posing challenges in coastal management and infrastructure planning. Furthermore, in these regions, the inelastic subsidence can disrupt natural drainage patterns, negatively affect the health of local habitats, and potentially cause increased saltwater intrusion into freshwater resources. These impacts highlight the necessity of studying inelastic subsidence in expansive soils, thereby guiding a comprehensive approach to urban development and environmental conservation. Unfortunately, to date, there have been few published studies on the inelastic deformation of expansive soils during drought events. The primary reason for this is the scarcity of long-term, in-situ data that precisely measure inelastic subsidence. Often, the minor inelastic subsidence is obscured by elastic subsidence and other forms of inelastic deformation.

This study aims to illuminate the often-overlooked phenomenon of inelastic subsidence in expansive soils, as recorded by advanced Global Positioning System (GPS) technology. Long-term, continuous, and precise measurements are crucial for accurately quantifying the extent of inelastic subsidence. The study examines the implications of the inelastic subsidence for coastal flooding, wetland and environmental conservation, infrastructure stability, and land and water resource management, with a particular focus on the coastal context of Galveston, Texas.

2. Data and Methods

2.1. Study Area

The Texas coastal area is home to the Beaumont Formation, which consists of Pleistocene-age sediments composed of fluvial and deltaic-plain clays and sands, stretching along the Texas coast. The Beaumont Formation can be further divided into two groups: areas predominantly composed of sand and areas predominantly composed of clay (Stoeser et al., 2005) (Figure 1). The latter, also known as Beaumont clay, consists of clay and mud deposits with low permeability and typically contains high percentages of smectite, contributing to the formation of expansive soils. In general, formations rich in clay are more prone to displaying swelling and shrinking characteristics compared to those primarily composed of sand. The thickness of the Beaumont Formation in the Texas coastal area varies by location, ranging from a few meters to over one hundred meters (Bureau of Economic Geology, 1992). The Houston-Galveston region faces numerous environmental and geotechnical challenges due to its location on expansive soils.

To understand the behavior of these expansive soils, we established a GPS array at the University of Houston Coastal Center (UHCC) in 2014 (Figure 2a). UHCC is located approximately 23 km from the Galveston coastline and is situated in an area covered by Beaumont clays. This array consists of four GPS stations, each with an antenna pole anchored at varying depths below the land surface. Specifically, the depths of the boreholes at UHC3, UHC2, and UHC1 are 10 m, 7 m, and 4 m below the land surface, respectively (Figure 2b). The bottoms of these antenna poles are anchored at the bases of the boreholes and are encased in PVC pipes. These PVC pipes act as sleeves, shielding the antenna poles from the forces associated with consolidating sediments. Consequently, the GPS antennas move in sync with the vertical movements of the sediments located beneath the bottom of the boreholes. In installing the cast-in-place concrete pad for UHC0, we excavated about two feet below the land surface, aiming to eliminate the influence of shallow soils with extensive roots and other materials. Our field observations indicate that during drought summers, the concrete pad of UHC0 exhibits consistent movement with the surrounding land surface. This array is meticulously designed to precisely measure soil compaction across various depths: 0–4 m, 4–7 m, 7–10 m, and below 10 m.

2.2. Data Processing Methods

GPS data processing methods generally utilize two approaches to achieve high-precision positions: relative and absolute positioning (e.g., Herring et al., 2016; Wang et al., 2017). The relative positioning relies on simultaneous observations from two or more GPS units to decide the relative position, specifically the three-component baseline lengths in the north-south (NS), east-west (EW), and up-down (UD) directions, between a rover antenna and a reference antenna. The baseline lengths are determined using the carrier-phase double difference method, commonly abbreviated as DD. The changes of the baseline length over time indicate the displacements of the rover antenna with respect to the reference antenna. In this study, the GAMIT/GLOBK software package (V.

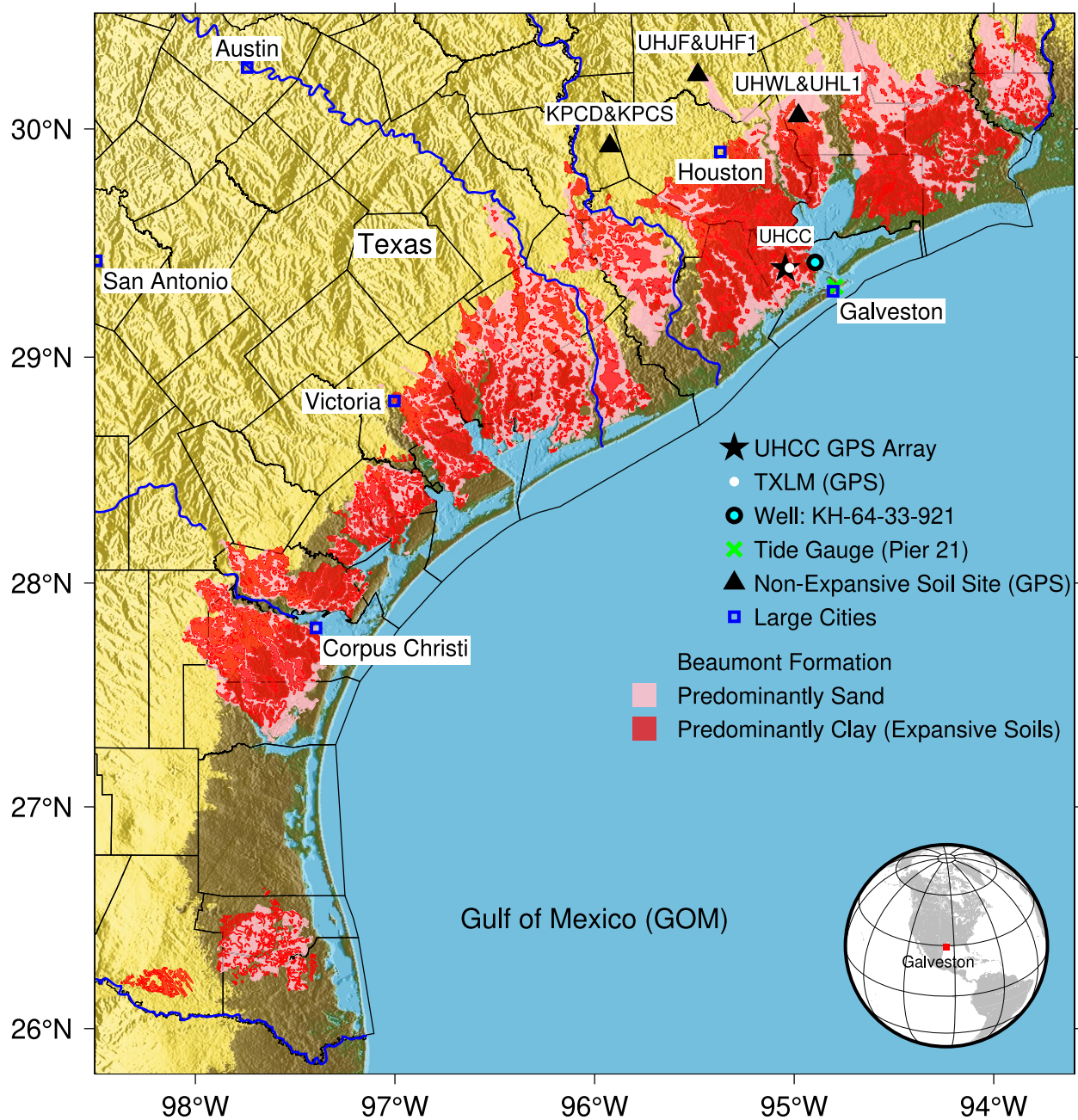


Figure 1. Locations of GPS stations used in this study and distribution of the Beaumont Formation in the Texas coastal region. The Beaumont Formation includes types that are predominantly clay or sand (Stoeser et al., 2005). The clay-dominant type is recognized for its significant swell-shrink behavior and is commonly referred to as expansive soils in geotechnical engineering.

10.71) is used for DD processing (Herring et al., 2020). For detailed information on the parameters used in the DD processing, please refer to Guo et al. (2019). According to our previous research, the DD method is capable of achieving sub-millimeter accuracy in terms of the root mean square (RMS) of daily displacements for extremely short baselines (e.g., <1 km) (e.g., Bao et al., 2018; Wang, 2012).

In contrast to relative positioning, the absolute positioning method requires only a single GPS station to determine its coordinates with respect to a global reference frame. Precise Point Positioning (PPP) is a commonly used absolute positioning method capable of achieving millimeter-level accuracy using a single GPS unit (Zumberge

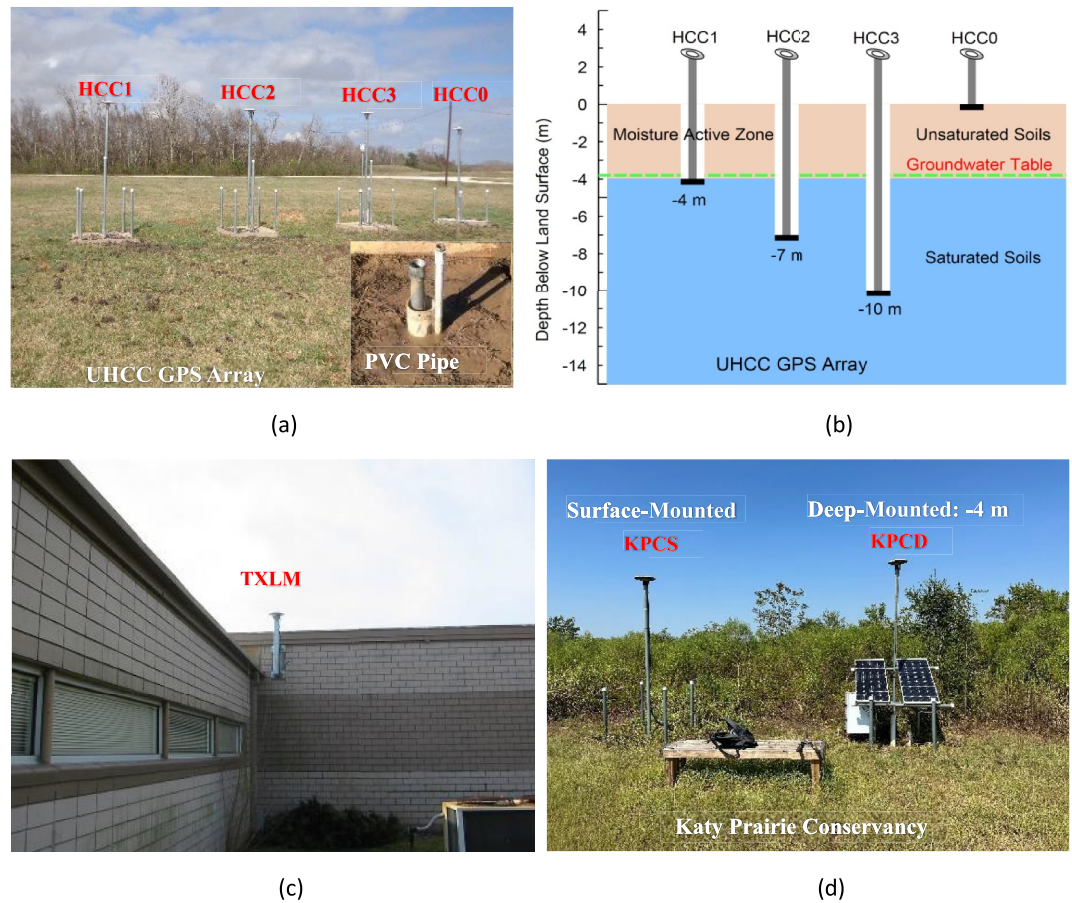


Figure 2. (a) An overview of the University of Houston Coastal Center (UHCC) GPS array positioned on expansive soils, (b) a schematic representation displaying the depths of GPS antenna poles, (c) the GPS antenna of TXLM, a Continuously Operating Reference Station (CORS) operated by the Texas Department of Transportation, situated on expansive soils, approximately 2 km east of UHCC, (d) GPS stations at Katy Prairie Conservancy: surface-mounted (KPCS) and deep-mounted (KPCD), situated on non-expansive soils.

et al., 1997). To delineate 24-hr average positions, also referred to as daily solutions, we utilize the single-receiver phase ambiguity-fixed PPP method integrated into the GipsyX software package (Bertiger et al., 2010, 2020). The initial coordinates for these daily solutions are aligned with the International GNSS Service Reference Frame 2014 (IGS14) (Rebischung et al., 2016). Detailed parameters for PPP processing are consistent with those used for the routine processing of the Houston GPS Network, as outlined in Wang et al. (2022). The daily PPP solutions achieve an approximate RMS-accuracy of 2–4 mm in the horizontal directions and 5–8 mm in the vertical direction within the Greater Houston region (Agudelo et al., 2020; Kearns et al., 2019).

Practically, interpreting site velocities with respect to a global reference frame can be challenging from a regional or local geophysical perspective. In this study, the coordinates of the PPP solutions, originally aligned with IGS14, are transformed to a regional reference frame, known as the Stable Gulf of Mexico Reference Frame 2020 (GOM20) (Wang et al., 2020).

3. Results and Discussions

3.1. PPP Solutions

Figure 3a depicts the vertical displacement time series derived from daily PPP solutions at the UHCC site and a nearby building-based GPS station (TXLM). TXLM is a permanent GPS station on a one-story office building (Figure 2c) located 2 km east of UHCC. While we do not have exact information on the depth of the building's

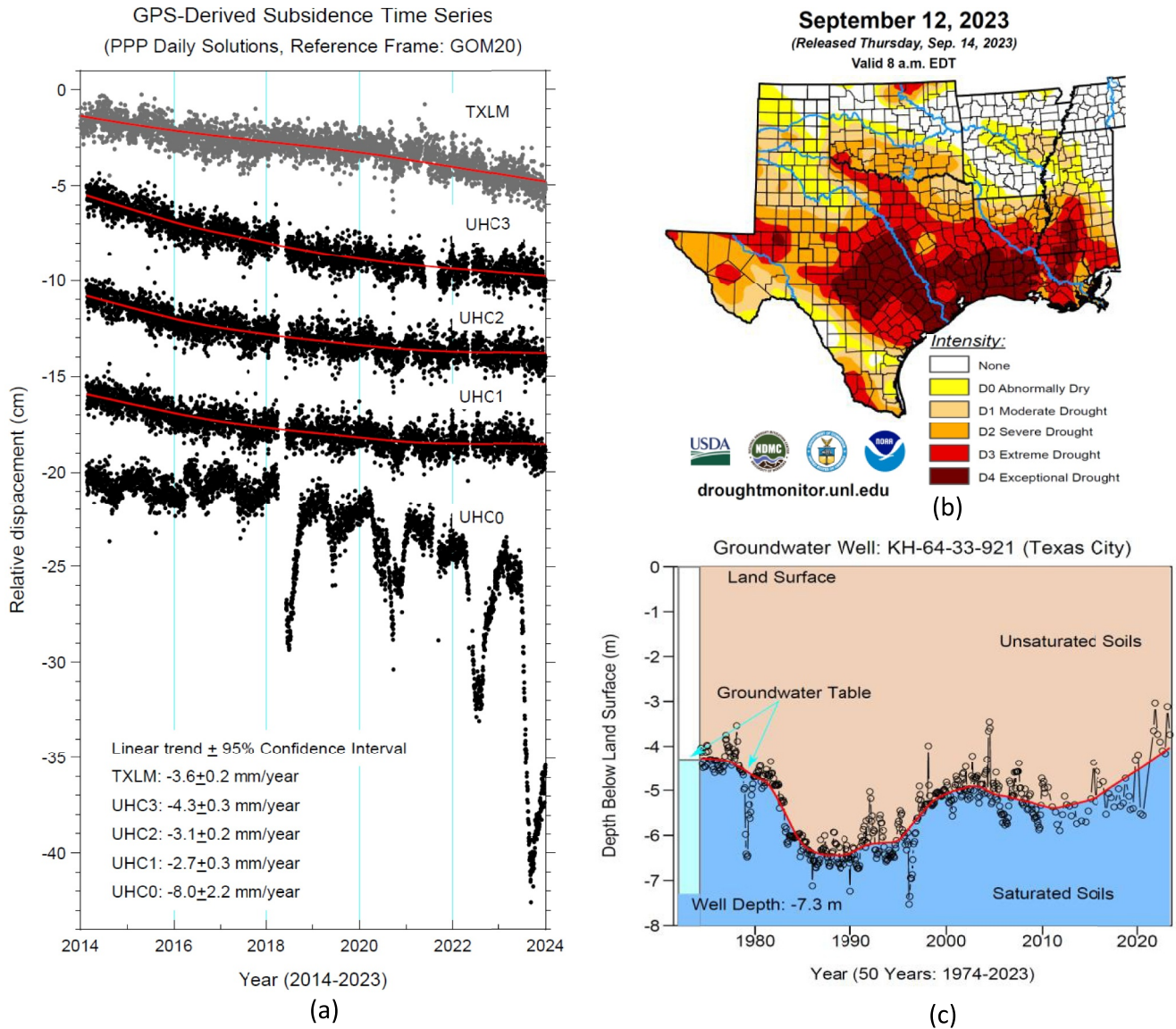


Figure 3. (a) Daily subsidence time series (PPP solutions) derived from GPS data at TXLM, UHC3, UHC2, UHC1, and UHC0, referenced to the GOM20 reference frame. Methods for calculating the average subsidence rate and its 95% confidence interval (95%CI) are detailed in Wang (2022b) and Cornelison and Wang (2023). (b) U.S. Drought Monitor map released on 14 September 2023 (map source: <https://droughtmonitor.unl.edu>). (c) The local groundwater table measurements recorded at a USGS groundwater well (Name: KH-64-33-921, ID: USGS-292458094534207, Well depth: 7.3 m below land surface) in Texas City, located 15 km to the east of the University of Houston Coastal Center (UHCC).

foundation, it is estimated to be within 2 m below land surface. In this study, only the GPS signals are used to determine the daily positions. There are occasional data gaps, mostly attributable to power supply failures in the field. The GPS stations at the UHCC site rely on onsite AC power for their operation. TXLM, UHC3, UHC2, and UHC1 exhibit a subsidence rate of 3–4 mm/year, which aligns with the ongoing natural subsidence rate in the Galveston coastal area (Zhou et al., 2021). Land subsidence due to groundwater withdrawals ceased in the early 2000s in this region (e.g., Greuter et al., 2021; Yu et al., 2014; Keans et al., 2015). Therefore, the ongoing permanent subsidence is primarily caused by the natural compaction of unconsolidated sediments, which are approximately 2000 m thick in this area (Zhou et al., 2021).

The subsidence time series at UHC0 reveals a noteworthy pattern of rapid subsidence during the summers of 2018, 2020, 2022, and 2023. The subsidence reached approximately 8 cm in the summer of 2018, 6 cm in the

summer of 2020, 8 cm in the summer of 2022, and 16 cm in the summer of 2023. Further investigations have solidified a compelling connection between this rapid subsidence and the prolonged drought conditions experienced during these summers. As per the U.S. Drought Monitor (<https://droughtmonitor.unl.edu>), the Houston-Galveston area endured a sequence of severe drought episodes during the past years. It commenced with moderate to severe drought conditions (D1 to D2) in early summer 2018, followed by an extended severe drought in 2020 (D2), intensifying to extreme drought (D3) during the summer of 2022, and culminating in an unparalleled exceptional drought (D4) in the summer of 2023 (Figure 3b).

Strong indications point to the substantial subsidence observed at UHC0 as a consequence of expansive soils contracting due to moisture loss during extended drought periods. Notably, the time series data reveals an almost complete restoration of the land surface to its pre-summer levels during the subsequent fall, coinciding with soil moisture restoration (rehydration) after the summer. This observation implies that the subsidence is primarily attributed to elastic deformation processes. UHC1, UHC2, and UHC3 exhibited no significant vertical deformation linked to the drought, indicating that the effects of droughts are predominantly confined to a depth within 4 m in this region.

TXLM exhibited no significant vertical subsidence during the drought events. This trend holds true for all HoustonNet GPS mounted on one-to two-story office or school buildings, as extensively documented in Wang (2022a). This phenomenon can be attributed to a combination of factors. First, soils beneath building foundations have been considered as integral components of foundation design, often fortified to mitigate potential issues arising from soil expansion and contraction. Second, building foundations and pavements themselves can serve as a protective barrier, effectively hindering excessive moisture loss in the soils beneath them during drought conditions. A crucial conclusion drawn from this study is that the impacts of drought on land subsidence are significantly less pronounced in built-up areas compared to open-field areas.

Figure 3c illustrates 50 years of groundwater level measurements (1974–2023) recorded in a shallow well located in Texas City, 15 km east of UHCC (Figure 1). The well is terminated in the Beaumont Formation and has a depth of 7.3 m below the land surface. These measurements define the concept of the groundwater table, which serves as the boundary between saturated and unsaturated zones beneath land surface. In areas above this table, pore spaces contain both air and water, also referred to as the moisture active zone. The depth of the water table varies seasonally, exhibiting a cyclical pattern. The groundwater table in this region has fluctuated between 4 and 6 m below the land surface over the past half-century. The most recent measurement, conducted in March 2023, recorded a groundwater table depth of 3.7 m below the land surface. While there is a clear seasonal pattern with higher levels in winter and lower levels in summer, the average amplitude of these fluctuations remains around one m. Notably, no significant drops in the groundwater table were observed during the prolonged droughts in the summers of 2018, 2020, and 2022. The stable groundwater table helps to explain why the impact of these drought events was limited to depths not exceeding 4 m below the land surface. The presence of a relatively stable local groundwater table ensures that the drying of shallow soils is halted at its level.

3.2. DD Solutions

To investigate the details of rapid subsidence during drought conditions at the land surface, we applied the DD method to process GPS data at UHCC, with UHC2 chosen as the reference station due to its complete dataset. Figure 4 illustrates vertical displacement time series for UHC0, UHC1, and UHC3 with respect to UHC2. Notably, minimal vertical displacement is observed between UHC2 and UHC3, with less than 5 mm over 10 years, and the displacement between UHC2 and UHC1 is almost zero during the same period. After experiencing significant subsidence, the land surface elevation did not fully recover, indicating inelastic subsidence during prolonged droughts. For example, UHC0 showed a total subsidence of approximately 8 cm during the summer of 2018, with 6 mm deemed inelastic, a similar pattern observed in the summer of 2022. In the summer of 2020, a drought that was less intense but more prolonged than those in 2018 and 2022 led to a total subsidence of around 7 cm, of which approximately 8 mm was inelastic. The magnitude of inelastic subsidence comprises about 10% of the total subsidence. The exceptional drought in the summer of 2023 caused 16-cm subsidence.

3.3. Drought-Induced Subsidence Versus Natural Subsidence

In general, shallow deposits with high organic and clay-rich facies tend to experience more rapid compaction than deeper and older sediments (e.g., Kareger et al., 2020; van Asselen et al., 2020; Keogh et al., 2021). It is crucial to

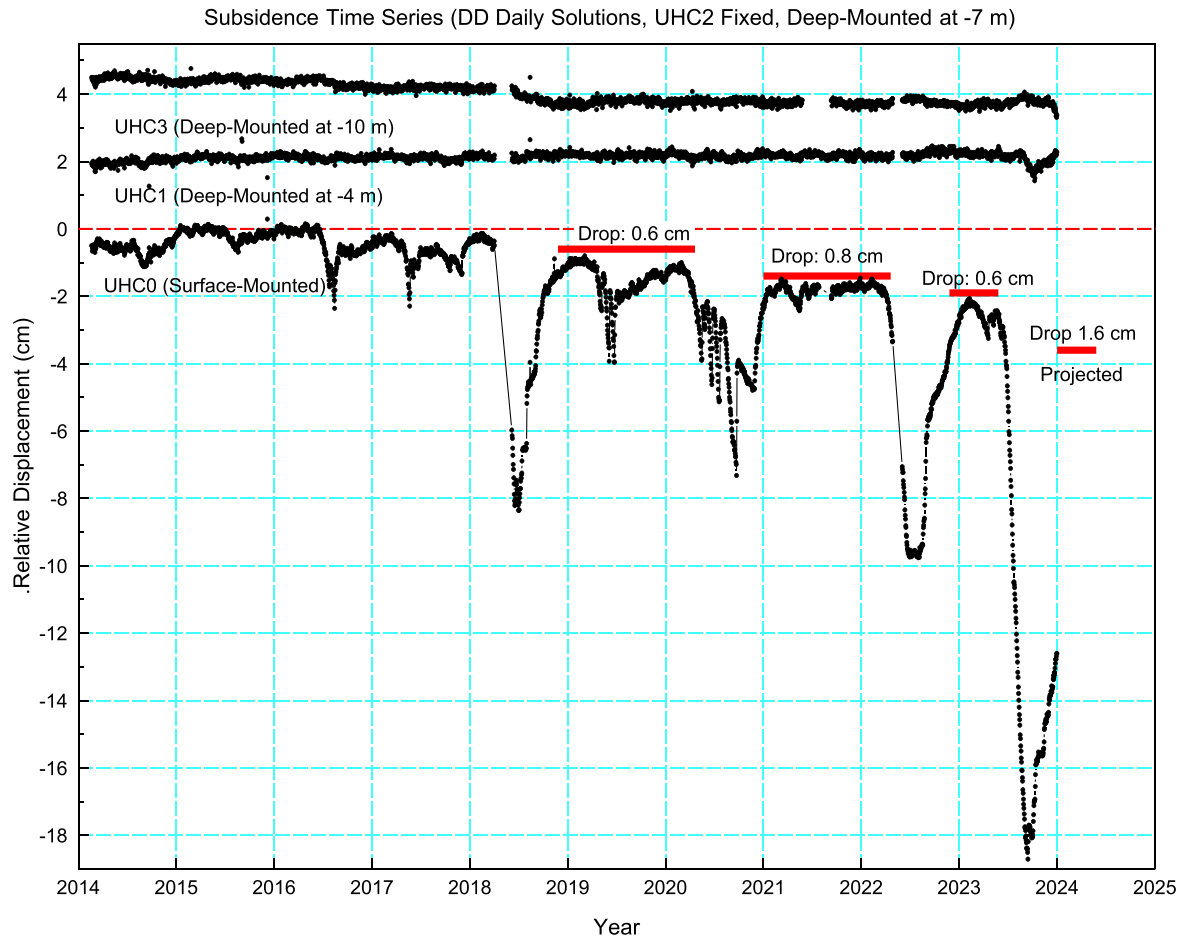


Figure 4. Vertical daily displacement time series (DD solutions) for GPS antennas at UHC0, UHC1, and UHC3, relative to the antenna at UHC2. The projected land surface elevation for the winter of 2023 is expected to be 1.6 cm lower than that of winter 2022, and 3.6 cm lower than that of winter 2017, assuming that inelastic compaction accounts for 10% of the total subsidence.

differentiate between drought-induced inelastic subsidence and the shallow subsidence observed within the uppermost few meters of strata. Shallow subsidence, such as that observed in the Mississippi Delta area, primarily results from the natural consolidation processes occurring in Holocene-aged sediments (e.g., Chamberlain et al., 2021; Törnqvist et al., 2008). Additionally, similar natural processes also occur within deeper, older unconsolidated sediments (e.g., Byrnes et al., 2019; Wang, 2023b; Zumberge et al., 2022).

Drought-induced inelastic subsidence often manifests as a step-like or discontinuous pattern of sinking. This pattern is marked by noticeable, permanent drops in land elevation during each drought period. In contrast, natural subsidence typically proceeds at a more steady or gradual pace over an extended period. Importantly, drought-induced inelastic subsidence is particularly significant in open-field areas but often goes unnoticed in built-up regions. This type of subsidence primarily occurs at a local scale, affecting specific areas with prevalent expansive soils where drought events significantly impact soil moisture content. Conversely, natural subsidence operates on a regional scale, affecting broader geographic areas and exhibiting more uniform and widespread effects across a region. Understanding these differences is vital for assessing subsidence risks in various coastal regions.

3.4. Non-Expansive Soils Versus Expansive Soils

To facilitate a comparative analysis between expansive soil areas and non-expansive soil areas with respect to drought impacts, additional GPS stations were strategically installed in non-expansive soil areas in the Greater

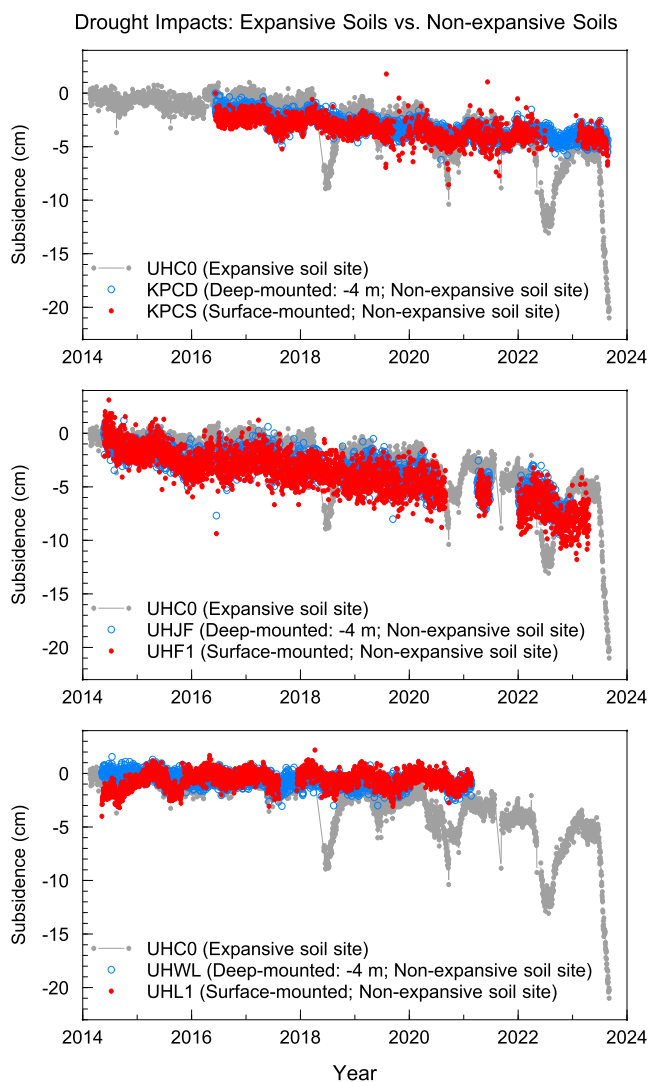


Figure 5. Comparisons of GPS-derived subsidence time series in expansive soil and non-expansive soil areas. The locations of these GPS stations are marked in Figure 1.

Houston region. These include the Katy Prairie Conservancy in Waller County (KPCD & KPCS), The W.G. Jones State Forest (abbreviated as Jones Forest) in Montgomery County (UHJF & UHF1), and West Liberty Airport in West Liberty County (UHWL & UHL1) (Figure 1). The Katy Prairie Conservancy site is situated on the Lissie Formation, which predominantly consists of sand and silt deposits, with geological ages ranging from the Middle Pleistocene to the Quaternary period. The Jones Forest site is located on the Willis Formation, primarily composed of gravel, sand, and silt, dating back to the Pliocene. The West Liberty Airport site is situated at the northern edge of the Beaumont Formation, predominantly comprising sand, with geological origins tracing back to the Late Pleistocene. All three sites are classified as areas with non-expansive soils.

A site photo showcasing the two GPS stations at the Katy Prairie Conservancy location is provided in Figure 2d. The antenna pole for GPS station KPCD is securely anchored at a depth of 4 m below the land surface, with a PVC pipe serving as a protective barrier. This design is similar to those employed at UHC1, UHC2, and UHC3. KPCS features an antenna pole mounted on a concrete pad at ground level. Both surface-mounted and deep-mounted GPS stations were deployed to provide precise soil compaction data within the 0 to 4-m depth range, as well as below 4 m.

Figure 5 displays the daily vertical displacement time series (PPP solutions) at these non-expansive soil sites. The positional scatter observed at UHJF and UHF1 in Jones Forest is notably greater than at other sites, primarily due to interference from the tall trees encircling the GPS stations. For comparison, the subsidence time series at UHC0 is also shown. Notably, the displacement time series recorded by both the surface-mounted and deep-mounted GPS units at each site are virtually indistinguishable. Furthermore, it is evident that the surface-mounted GPS units at these locations were minimally affected by the droughts occurring in the summer months, underscoring the limited impact of droughts in non-expansive soil regions.

4. Implications

4.1. Relative Sea-Level Rise and Coastal Flooding

Sea-level rise, driven by climate change, combined with vertical land movements, influences coastal flooding assessments. Traditional methods using benchmarks or GPS, often attached to deep structures, overlook the permanent compaction of shallow soils. This oversight might underestimate relative sea-level rise rates (e.g., Jankowski et al., 2017; Keogh & Törnqvist, 2019; Wang, 2022a).

At UHCC, inelastic subsidence over 10 years added 3.6 mm/year to vertical land movement (Figure 4). On Galveston Island, one long-standing tide gauge station, Galveston Pier 21 (1908–2023) (see Figure 1), recorded a 6.6 mm/year relative sea-level rise (Wang, 2023a), combining sea-level rise (2.6 mm/year) and natural subsidence (4.0 mm/year) (Wang et al., 2020; Zhou et al., 2021). This study finds that relative sea-level rise rates in developed coastal areas are likely lower than in undeveloped areas with expansive soils. The omission of inelastic subsidence in coastal flood projections could downplay actual flood risks, especially with increasing droughts under climate change. Accurately accounting for inelastic subsidence is vital for realistic future flood risk assessments.

4.2. Coastal Wetland Losses and Gains

The Texas coastal region contains millions of acres of wetlands of varying types, which overlay expansive soils. These wetlands play crucial roles in biodiversity, sediment stabilization, flood attenuation, and water purification. In general, land subsidence increases water depths in wetlands over time, contributing to the conversion of

vegetated coastal wetlands to either open water or shallow subaqueous flats. This makes them less suitable for certain plant and animal species (e.g., Cahoon, 2015; Kolker et al., 2011; Reed, 2002; White & Tremblay, 1995). This process is commonly known as wetland losses. Drought-induced subsidence differs from regional and continuous subsidence. It occurs only in areas not covered by water during summers. Following repeated drought events, significant inelastic subsidence can accumulate in areas adjacent to wetlands that are not typically covered by water. As a result, this inelastic subsidence can create depressions in the landscape capable of collecting water, a process known as wetland gains, leading to the creation or enlargement of wetland areas. However, it is also plausible that the inelastic subsidence may transform previously existing wetlands into open water areas, thereby converting terrestrial ecosystems into aquatic expanses and effectively reducing the overall size of the wetland. Understanding the dual impact of inelastic subsidence on wetlands is crucial for effective coastal wetland management.

4.3. Calibration of Interferometric Synthetic Aperture Radar (InSAR) Using GPS

GPS-derived ground deformation time series, often used to calibrate and verify InSAR-derived land surface deformation, typically come from stations on buildings or deeply mounted monuments, which miss inelastic deformation in shallow soils (Yang et al., 2016). InSAR, however, specializes in surface deformation measurement. Thus, subsidence rates from GPS and InSAR can differ significantly, especially in open fields with undisturbed expansive soils. Researchers need to be aware of these potential disparities in GPS and InSAR data comparisons.

4.4. Engineering Challenges

Expansive soils present complex challenges for infrastructure design and planning, with current engineering practices mainly focusing on elastic deformation like seasonal heave and subsidence. This study underscores the often-neglected cumulative impact of repeated droughts, causing significant inelastic compaction in shallow soils. Such changes can affect local topography, altering drainage, water retention, and flood risk. Understanding the relationship between drought patterns, groundwater levels, and subsidence extent is vital for assessing infrastructure risks and urban planning.

5. Conclusions

The decade-long GPS datasets from UHCC reveal that prolonged droughts have the potential to induce significant subsidence in open-field areas situated on expansive soils. Typically, the deformation of expansive soils is limited to a shallow depth above the local groundwater table, not exceeding 4 m in the Galveston coastal region. During recent drought events, the subsidence at the UHCC was up to two dm, with inelastic subsidence accounting for approximately 10% of the total subsidence.

Inelastic subsidence, often overlooked in areas with expansive soils, has far-reaching implications, especially in the context of prolonged droughts and climate changes. It significantly affects land surface elevation and challenges traditional methods of assessing sea-level rise, potentially leading to an underestimation of coastal flooding risks. This revelation is crucial for both scientists and engineers. For scientists, it deepens the understanding of how meteorological conditions interact with soil and groundwater. For engineers and urban planners, it emphasizes the need to consider inelastic subsidence in coastal infrastructure projects. Growing awareness in this field may inspire more focused research and the development of effective mitigation strategies.

Conflict of Interest

The authors declare no conflicts of interest relevant to this study.

Data Availability Statement

The GPS data at UHCC sites were sourced from UNAVCO (<https://www.unavco.org/data/gps-gnss/data-access-methods/gnss-data-access-notebook/gnss-data-access-notebook.html>) and the GPS data at TXLM were sourced from National Geodetic Survey (https://geodesy.noaa.gov/cgi-cors/corsage_2.pr1?site=TXLM). Groundwater data were obtained from the USGS National Water Information System (NWIS) Mapper (<https://maps.waterdata.usgs.gov/mapper/index.html>).

Acknowledgments

The installation and operation of the GPS stations utilized in this study benefited from the participation of numerous graduate and undergraduate students at the University of Houston, whose contributions are gratefully acknowledged. Special thanks are extended to Dr. Timothy J. Keans, a graduate from the University of Houston who earned his Ph.D. in 2018, for playing an important role in installing the GPS stations. The authors also extend their appreciation to Hans Williamson, David Maggert, and Jim Normandeau for archiving GPS data at UNAVCO. The authors are grateful for the insightful feedback provided by two anonymous reviewers.

References

- Agudelo, G., Wang, G., Liu, Y., Bao, Y., & Turco, M. J. (2020). GPS geodetic infrastructure for subsidence and fault monitoring in Houston, Texas, USA. *Proceedings of the IAHS*, 382, 11–18. <https://doi.org/10.5194/piahs-382-11-2020>
- Bao, Y., Guo, W., Wang, G., Gan, W., Zhang, M., & Shen, S. (2018). Millimeter-accuracy structural deformation monitoring using standalone GPS: Case study in Beijing, China. *Journal of Surveying Engineering*, 144(1), 05017007. [https://doi.org/10.1061/\(ASCE\)SU.1943-5428.0000242](https://doi.org/10.1061/(ASCE)SU.1943-5428.0000242)
- Barthélémy, S., Bonan, B., Calvet, J.-C., Grandjean, G., Moncoulon, D., Kapsambelis, D., & Bernardie, S. (2023). A new drought index fitted to clay shrinkage induced subsidence over France: Benefits of interactive leaf area index. *EGU sphere*. <https://doi.org/10.5194/egusphere-2023-1366>
- Bertiger, W., Bar-Sever, Y., Dorsey, A., Haines, B., Harvey, N., Hemberger, D., et al. (2020). GipsyX/RTGx, a new tool set for space geodetic operations and research. *Advances in Space Research*, 66(3), 469–489. <https://doi.org/10.1016/j.asr.2020.04.015>
- Bertiger, W., Desai, S., Haines, B., Harvey, N., Moore, A., Owen, S., & Weiss, J. (2010). Single receiver phase ambiguity resolution with GPS data. *Journal of Geodesy*, 84(5), 327–337. <https://doi.org/10.1007/s00190-010-0371-9>
- Bureau of Economic Geology. (1992). *Geologic Map of Texas*. University of Texas at Austin. Virgil E. Barnes, project supervisor, Hartmann, B. M. and Scranton, D.F., cartography, scale 1:500,000.
- Byrnes, M. R., Britsch, L. D., Berlinghoff, J. L., Johnson, R., & Khalil, S. (2019). Recent subsidence rates for Barataria Basin, Louisiana. *Geo-Marine Letters*, 39(4), 265–278. <https://doi.org/10.1007/s00367-019-00573-3>
- Cahoon, D. R. (2015). Estimating relative sea-level rise and submergence potential at a coastal wetland. *Estuaries and Coasts*, 38(3), 1077–1084. <https://doi.org/10.1007/s12237-014-9872-8>
- Chamberlain, E. L., Shen, Z., Kim, W., McKinley, S., Anderson, S., & Törnqvist, T. E. (2021). Does load-induced shallow subsidence inhibit delta growth? *Journal of Geophysical Research: Earth Surface*, 126(11), e2021JF006153. <https://doi.org/10.1029/2021JF006153>
- Charpentier, A., James, M., & Ali, H. (2022). Predicting drought and subsidence risks in France. *Natural Hazards and Earth System Sciences*, 22(7), 2401–2418. <https://doi.org/10.5194/nhess-22-2401-2022>
- Cornelson, B., & Wang, G. (2023). GNSS_Vel_95CI.py: A Python Module for calculating the uncertainty of GNSS-derived site velocity. *Geophysical Research Letters*, 149(1), 06022001. [https://doi.org/10.1061/\(ASCE\)SU.1943-5428.0000410](https://doi.org/10.1061/(ASCE)SU.1943-5428.0000410)
- Greuter, A., Turco, M. J., Petersen, C. M., & Wang, G. (2021). Impacts of groundwater withdrawal regulation on subsidence in Harris and Galveston Counties, Texas, 1978–2020. *GeoGulf Transactions*, 71, 109–118.
- Guo, W., Wang, G., Bao, Y., Li, P., Zhang, M., Gong, M., et al. (2019). Detection and monitoring of tunneling-induced riverbed deformation using GPS and BeiDou: A case study. *Applied Sciences*, 9(13), 2759. <https://doi.org/10.3390/app9132759>
- Herring, T. A., King, R. W., Floyd, M. A., & McClusky, S. C. (2020). *Introduction to GAMIT/GLOBK (V. 10.7)*. Department of Earth, Atmospheric and Planetary Sciences. Massachusetts Institute of Technology. Retrieved from <http://geoweb.mit.edu/gg/>
- Herring, T. A., Melbourne, T. I., Murray, M. H., Floyd, M. A., Szeliga, W. M., King, R. W., et al. (2016). Plate boundary observatory and related networks: GPS data analysis methods and geodetic products. *Reviews of Geophysics*, 54(4), 759–808. <https://doi.org/10.1002/2016RG000529>
- Jankowski, K. L., Törnqvist, T. E., & Fernandes, A. M. (2017). Vulnerability of Louisiana's coastal wetlands to present-day rates of relative sea-level rise. *Nature Communications*, 8(1), 14792. <https://doi.org/10.1038/ncomms14792>
- Kai, L., Liang, K., Hossein, N., & Cyrille, C. (2020). The mechanical behavior of an expansive soil due to long-term seasonal rainfalls. *E3S Web of Conferences*, 195, 02019. <https://doi.org/10.1051/e3sconf/202019502019>
- Karegar, M. A., Larson, K. M., Kusche, J., & Dixon, T. H. (2020). Novel quantification of shallow sediment compaction by GPS interferometric reflectometry and implications for flood susceptibility. *Geophysical Research Letters*, 47(14), e2020GL087807. <https://doi.org/10.1029/2020gl087807>
- Keans, T. J., Wang, G., Bao, Y., Jiang, J., & Lee, D. (2015). Current land subsidence and groundwater level changes in the Houston metropolitan area (2005–2012). *Journal of Surveying Engineering*, 141(4), 05015002. [https://doi.org/10.1061/\(ASCE\)SU.1943-5428.0000147](https://doi.org/10.1061/(ASCE)SU.1943-5428.0000147)
- Keans, T. J., Wang, G., Turco, M., Welch, J., Tsibanos, V., & Liu, H. (2019). Houston16: A stable geodetic reference frame for subsidence and faulting study in the Houston metropolitan area, Texas, U.S. *Geodesy and Geodynamics*, 10(5), 382–393. <https://doi.org/10.1016/j.geog.2018.05.005>
- Keogh, M. E., & Törnqvist, T. E. (2019). Measuring rates of present-day relative sea-level rise in low-elevation coastal zones: A critical evaluation. *Ocean Science*, 15(1), 61–73. <https://doi.org/10.5194/os-15-61-2019>
- Keogh, M. E., Törnqvist, T. E., Kolker, A. S., Erkens, G., & Bridgeman, J. G. (2021). Organic-matter accretion, shallow subsidence, and river delta sustainability. *Journal of Geophysical Research: Earth Surface*, 126(12), e2021JF006231. <https://doi.org/10.1029/2021jfo06231>
- Kolker, A. S., Allison, M. A., & Hameed, S. (2011). An evaluation of subsidence rates and sea-level variability in the northern Gulf of Mexico. *Geophysical Research Letters*, 38(21). <https://doi.org/10.1029/2011GL049458>
- Mostafiz, R. B., Friedland, C. J., Rohli, R. V., Bushra, N., & Held, C. L. (2021). Property risk assessment for expansive soils in Louisiana. *Frontiers in Built Environment*, 7, 1–10. <https://doi.org/10.3389/fbuil.2021.754761>
- Rebischung, P., Altamimi, Z., Ray, J., & Garayt, B. (2016). The IGS contribution to ITRF2014. *Journal of Geodesy*, 90(7), 611–630. <https://doi.org/10.1007/s00190-016-0897-6>
- Reed, D. J. (2002). Sea-level rise and coastal marsh sustainability: Geological and ecological factors in the Mississippi delta plain. *Geomorphology*, 48(1–3), 233–243. [https://doi.org/10.1016/S0169-555X\(02\)00183-6](https://doi.org/10.1016/S0169-555X(02)00183-6)
- Stoeser, D. B., Green, G. N., Morath, L. C., Heran, W. D., Wilson, A. B., Moore, D. W., & Van Gosen, B. S. (2005). Preliminary integrated geologic map databases for the United States *USGS Open-File Report*. pp. 2005–1351, Retrieved from <https://pubs.usgs.gov/of/2005/1351/>
- Törnqvist, T. E., Wallace, D. J., Storms, J., Wallinga, J., van Dam, R. L., Blauw, M., et al. (2008). Mississippi delta subsidence primarily caused by compaction of Holocene strata. *Nature Geoscience*, 1(3), 173–176. <https://doi.org/10.1038/ngeo129>
- van Asselen, S., Erkens, G., & de Graaf, F. (2020). Monitoring shallow subsidence in cultivated peatlands. *Proceedings of the IAHS*, 382, 189–194. <https://doi.org/10.5194/piahs-382-189-2020>
- Wang, G. (2012). Kinematics of the Cerca del Cielo, Puerto Rico landslide derived from GPS observations. *Landslides*, 9(1), 117–130. <https://doi.org/10.1007/s10346-011-0277-5>
- Wang, G. (2022a). Seasonal subsidence and heave recorded by borehole extensometers in Houston. *Journal of Surveying Engineering*, 149(1), 04022018. <https://doi.org/10.1061/JSUED2.SUENG-1369>
- Wang, G. (2022b). The 95% confidence interval for the GNSS-derived site velocities. *Journal of Surveying Engineering*, 148(1), 04021030. [https://doi.org/10.1061/\(ASCE\)SU.1943-5428.0000390](https://doi.org/10.1061/(ASCE)SU.1943-5428.0000390)
- Wang, G. (2023a). The 95 per cent confidence interval for the mean sea-level change rate derived from tide gauge data. *Geophysical Journal International*, 235(2), 1420–1433. <https://doi.org/10.1093/gji/ggad311>

- Wang, G. (2023b). New preconsolidation heads following the long-term hydraulic-head decline and recovery in Houston, Texas. *Ground Water*, 61(5), 674–691. <https://doi.org/10.1111/gwat.13271>
- Wang, G., Greuter, A., Petersen, C. M., & Turco, M. J. (2022). Houston GNSS network (HoustonNet) for subsidence and faulting monitoring: Data analysis methods and products. *Journal of Surveying Engineering*, 148(4), 04022008. [https://doi.org/10.1061/\(ASCE\)SU.1943-5428.0000399](https://doi.org/10.1061/(ASCE)SU.1943-5428.0000399)
- Wang, G., Turco, M., Soler, T., Kearns, T., & Welch, J. (2017). Comparisons of OPUS and PPP solutions for subsidence monitoring in the greater Houston area. *Journal of Surveying Engineering*, 143(4), 05017005. [https://doi.org/10.1061/\(ASCE\)SU.1943-5428.0000241](https://doi.org/10.1061/(ASCE)SU.1943-5428.0000241)
- Wang, G., Zhou, X., Wang, K., Ke, X., Zhang, Y., Zhao, R., & Bao, Y. (2020). GOM20: A stable geodetic reference frame for subsidence, faulting, and sea-level rise studies along the coast of the Gulf of Mexico. *Remote Sensing*, 12(3), 350. <https://doi.org/10.3390/rs12030350>
- White, W. A., & Tremblay, T. A. (1995). Submergence of wetlands as a result of human-induced subsidence and faulting along the upper Texas Gulf Coast. *Journal of Coastal Research*, 11(3), 788–807. <http://www.jstor.org/stable/4298381>
- Yang, L., Wang, G., Bao, Y., Kearns, T. J., & Yu, J. (2016). Comparisons of ground-based and building-based CORS: A case study in the region of Puerto Rico and the Virgin Islands. *Journal of Surveying Engineering*, 142(3), 05015006. [https://doi.org/10.1061/\(ASCE\)SU.1943-5428.0000155](https://doi.org/10.1061/(ASCE)SU.1943-5428.0000155)
- Yu, J., Wang, G., Kearns, T. J., & Yang, L. (2014). Is there deep-seated subsidence in the Houston-Galveston area? *Journal of Geophysics*, 2014(1), 1–11. <https://doi.org/10.1155/2014/942834>
- Zhou, X., Wang, G., Wang, K., Liu, H., Lyu, H., & Turco, M. J. (2021). Rates of natural subsidence and submergence along the Texas coast derived from GPS and tide gauge measurements (1904–2020). *Journal of Surveying Engineering*, 147(4), 04021020. [https://doi.org/10.1061/\(ASCE\)SU.1943-5428.0000371](https://doi.org/10.1061/(ASCE)SU.1943-5428.0000371)
- Zumberge, J. F., Heflin, M. B., Jefferson, D. C., Watkins, M. M., & Webb, F. H. (1997). Precise point positioning for the efficient and robust analysis of GPS data from large networks. *Journal of Geophysical Research (Solid Earth)*, 102(B3), 5005–5017. <https://doi.org/10.1029/96JB03860>
- Zumberge, M. A., Xie, S., Wyatt, F. K., Steckler, M. S., Li, G., Hatfield, W., et al. (2022). Novel integration of geodetic and geologic methods for high-resolution monitoring of subsidence in the Mississippi Delta. *Journal of Geophysical Research: Earth Surface*, 127(9), e2022JF006718. <https://doi.org/10.1029/2022JF006718>